

ONGOING DEVELOPMENT OF SATELLITE-DERIVED WINDS AT NESDIS/CIMSS

C. M. Hayden

NOAA/NESDIS

Madison, Wisconsin USA

S. J. Nieman and T. J. Schmit

Cooperative Institute for Meteorological Satellite Studies

Madison, Wisconsin USA

1. INTRODUCTION

Research in the development of wind estimates from geostationary satellite imagery has been reported in Hayden and Merrill (1988), Merrill (1989), Hayden (1991), and Hayden et. al. (1992). These references describe many of the automated techniques currently used by the National Environmental Satellite and Data Distribution Service (NESDIS) for deriving vectors from consecutive images of the cloud (water vapor) observed with the GOES satellites. Included are explanations of the target selection method, the height assignment (see also Nieman et al., 1993), and the tracking algorithm which continues to be the maximization of correlation between an initial target sector and displaced sectors on a second (and third) image. Experimental studies investigating the suitability of combining the correlation function with a penalty function based on the error covariance of the "first guess" displacement were reported in Hayden and Merrill (1992). However, the additional complexity did not appear to offer any substantive improvement in the product, and the additional penalty function was never incorporated into operational methods.

The majority of our research effort in the last two years has been directed to further study of water vapor motions, development of cloud pressure-altitude assignment using the 6.7 micrometer channel, further evaluation of the objective quality control system for cloud motion vectors (CMV), which includes pressure altitude reassignment via assimilation with other data. In addition, we have considerably refined and automated our verification procedures to improve product monitoring for all operational satellite derived winds. We have also put more attention to the generation and evaluation of gradient winds using the temperature/moisture profiles derived from VAS. This now is also an operational product. These subjects will be treated individually in the following five sections. A final section summarizes the results, highlights persistent problems, and outlines current avenues of research.

2. WATER VAPOR MOTIONS

The possibility of a no-GOES environment occasioned by continuing delay in the launch of GOES-I and the aging of the remaining GOES-7 encouraged an agreement to move the METEOSAT-3 first to 50 and then to 75 W (early 1993). The improved, as compared to GOES-7, resolution (approximately 5 instead of 14 km) with only modestly degraded field-of view (fov) signal-to-noise (.7 vs. .5) in the water vapor band make these data attractive for further investigation of water vapor tracking. During the spring of 1992, wind sets were produced on a daily basis at the Cooperative Institute for Meteorological Satellite Studies (CIMSS). Unlike the EUMETSAT processing we have chosen to avoid cloud tracers (by requiring a minimum brightness temperature greater than 228 K) and concentrate on the cloud-free areas in the imagery. Height assignments are made using the histogram method, whereby an average 6.7 micrometer brightness temperature is matched to the temperature profile of the NMC forecast. These heights are susceptible to reassignment by the objective editor, and typically a far greater percentage are reassigned as compared to the GOES cloud drift winds which use the CO₂ slicing technique (Hayden et al. 1992). Accuracy, as determined by rawinsonde co-location statistics (Velden, 1993) has proven good enough to consider operational implementation, and four experimental water vapor wind sets are currently produced daily at the NESDIS processing. A discussion of the current accuracy will be given in section 5.

3. HEIGHT ASSIGNMENT USING THE WATER VAPOR BAND

It is anticipated that NESDIS will operationally process infrared CMV from the Meteosat-3 or -5 beginning in February, 1994. Because the 13.7 micrometer channel required in CO₂ height assignment is not available on these satellites (or on the upcoming GOES-I imager) an alternative method using the 6.7 micrometer channel has been investigated (Nieman et al. 1993). CIMSS has adopted a variation of the EUMETSAT approach (Szejwach, 1983) which compares measurements of the water vapor and infrared window in order to account for varying cloud emissivity. One part of the technique includes a clustering algorithm which identifies clusters in a plot of the 6.7 vs. the 11 micrometer window radiances for the 225 measurements included in a target sector. The members of each clusters are presumably affected by the same cloud type. A straight line (Fig. 1) is connected to the average radiances of the warmest and coldest clusters, forcing the relationship that radiance varies linearly with varying cloud amount (but not with varying cloud height and hence the clustering). A second part of the technique involves the calculation of radiances for both bands from a forecast temperature/moisture profile. Applying opaque cloud at at each pressure level of the profile yields a curve in the plot of 6.7 vs. 11 micrometer radiances. The points where the theoretical curve and the observational straight line intersect represent the cloud-free and overcast situation (see Fig. 1). The 11 micrometer radiance of the

latter is converted to a radiance temperature, and this is matched to the forecast temperature profile to determine a final cloud altitude.

Our experience has been that the cluster height assignment is inferior to the CO₂ slicing method (Nieman et al., 1993). Part of the difficulty lies with the flat slope of the theoretical curve at warmer temperatures causing the method to be insensitive with lower cloud. A further problem is an unknown bias in the forward calculated radiance at 6.7 micrometers relative to the observation. In practice an attempt is made to correct for the bias error by fitting the theoretical curve to the observations at the warm end, but this is a rather uncertain procedure. Referring to the bottom panels of Fig. 1 a pernicious problem with this technique is seen. In adjusting for the bias, at the warm scene, we are in an area of the Ch-3 (6.7) Planck curve where radiance is varying very rapidly with temperature, amplifying the effect of noise/uncertainty in picking the radiance adjustment. In applying that change at the cold scene, we are in an area of the Ch-4 (11) curve where radiance is varying slowly with temperature, amplifying the effect of noise/uncertainty in defining scene temperature. We have the worst of both worlds.

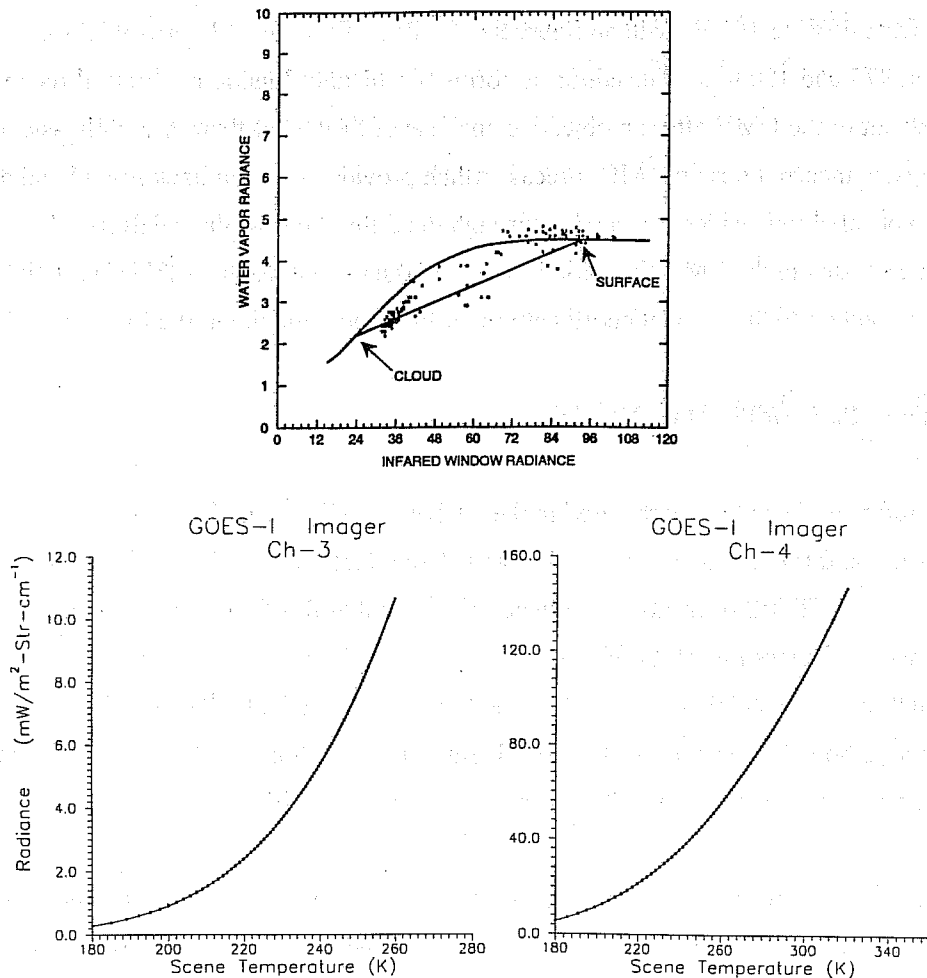


Fig. 1: Top: A schematic representation of the water vapor-infrared window method for assigning cloud pressure altitude. Planck relationships for the two channels are shown at the bottom.

Radiance bias is routinely monitored (in monthly samples) for the GOES-7 6.7 micrometer channel, as part of the VAS temperature/moisture retrieval processing. It varies randomly, but can amount to as much as half a unit of radiance for clear samples. Thus the line shown in Fig. 1 might be moved up or down by this amount. For colder (higher) clouds the associated change in the window radiance of the intercept may vary by as much as six counts, or approximately 8 K in radiance temperature. The error induced in the final cloud height will depend on the temperature lapse rate, but can amount to 50 hPa or more. In any event, the cluster algorithm is being applied routinely to operational processing of the Meteosat cloud-drift winds, and results are evaluated in Section 5.

4. QUALITY ESTIMATION AND HEIGHT REASSIGNMENT

Since February 1993 an auto-editor has been applied to the operationally processed cloud-drift winds. The formulation is discussed in Hayden (1991) and Hayden and Velden (1991). It is based on a 3-dimensional recursive filter objective analysis (Hayden and Purser, 1988). The analysis extends over 60 S to 60 N and from 45W to 165 W with an intervals of 2 deg. There are 13 vertical levels distributed between 975 and 100 hPa. The editor performs two distinct functions. First, it reconsiders the altitude assignment of the CMV after an objective analysis of the data at their originally assigned pressure. The analysis incorporates an NMC forecast which provides an initial background and also contributes pseudo observations which are carried through the 5 iterations of the analysis. The forecast is the same as used in the CMV derivation. In the reassignment, each CMV is "best-fit" to the initial analysis by moving it in the vertical coordinate (pressure) and minimizing the function:

$$(T_a - T)^2/dT^2 + (P_a - P)^2/dP^2 + (V_a - V)^2/dV^2 \quad (1)$$

where subscript a refers to the value interpolated in the analysis and T, P, and V are the cloud temperature, pressure, and vector respectively. The normalizing factors dT, dP, and dV are specified to be 10, 100, and 2 for NESDIS operational applications. Note that this "equates" a velocity discrepancy of 2 ms⁻¹ to a pressure reassignment of 100 hPa or a temperature change of 10K. The vertical search is limited between 900 hPa and the tropopause (as indicated by the analysis). Currently there is no limitation to how far a vector can be moved, but in practice this is limited by the T and P terms. A vector is rejected if the minimum fit exceeds a threshold, currently 50.

The second function of the editor is to provide a quality flag. This is obtained from a second objective analysis of the data at the reassigned pressures. A threshold is used to determine data which are not passed to the user. In neither preliminary nor final analysis are any data other than the CMV (and the forecast) used.

In addition to the tunable parameters included in the penalty function (1) and the choice of rejection threshold, there are a number of parameters in the analysis algorithm which can affect the relative influence of the background (NMC forecast) information and the data. Foremost among these are: the degree of smoothing assigned; error tolerance; and weight assigned to the background. Our goal has been to examine the sensitivity of the many parameters with respect to minimizing the error between the accepted (and possibly reassigned) cloud vectors and co-located rawinsondes. After some relatively exhaustive investigation we have arrived at three conclusions which are somewhat at odds with one another:

- o Best statistics are achieved by relying heavily on the initial analysis of velocity in reassessing the height. That is, it would appear favorable to fit tightly to the velocity and allow large deviations from the initial cloud pressure and temperature assignment.

- o As the influence of the velocity term in (1) is increased, the effectiveness of the quality threshold in discriminating bad vectors diminishes. This is logically consistent since the data are being forced to fit the preliminary analysis and therefore will in general receive high quality assessment in the final analysis. If we choose to permit large pressure (temperature) deviations we may ignore the threshold flagging.

However:

- o As the influence of the velocity term in (1) is increased, the change in altitude assignment becomes much larger than is reasonable.

Table 1 contains an example of match-up statistics (for one wind set) where the function (1) has been varied to reduce the dependence on initial temperature and pressure. It is clear that the numbers given for the 12 hr forecast support the first conclusion above. An improvement of 0.5 ms^{-1} is obtained as the operational variables are changed to emphasize only the velocity variable (Case 2 vs. Case 4). The second conclusion is also supported where the full sample of comparisons (69) shows no degradation over the thresholded sample (64) (Case 5 vs. Case 4). But the table also indicates that the standard deviation of original vs. reassigned pressure for the vectors grows from 59 hPa for the operationally used set (Case 2) to 180 hPa for Case 4. Since there is reason to believe that the CO₂ slicing method has an accuracy of about 50 hPa (Menzel, 1983), conclusion 3 is also justified.

A close look at 12 - hr results of Table 1 suggests that perhaps the reason the rms statistics improve as the velocity term of (1) is increased is because the forecast is initially more accurate than the wind vector. The forecast, serving as a background field, has a strong influence on the initial analysis, and reducing the influence of the temperature and pressure terms in (1) will drive the solution to the

background field. This cannot of course explain why the vectors eventually become more accurate than the background; this must be the influence of the vectors themselves in the initial analysis. It is certainly not desirable to allow the background too much influence, as this reduces the independence of the CMV observations. We need to be able to define the point of diminishing returns.

Table 1: Vector rms statistics comparing cloud drift wind and rawinsondes as "best-fit" function for altitude reassignment is varied. Results are shown for system operating with 12 and 60 hour forecast fields. Rms statistics (ms^{-1}) are the comparison with rawinsondes within 2 deg. latitude. Also shown is the standard deviation of the altitude reassignment, Sigp (hPa)

Case	dV	dT	dP	12-hr				60-hr			
				CMV	Fcst	N	SigP	CMV	Fcst	N	Sigp
1	-	-	-	9.3	7.4	63	-	10.9	10.2	66	-
2	2	10	100	7.5	7.3	57	59	9.1	9.9	55	74
3	2	10	1000	7.3	7.3	57	80	9.2	10.0	54	97
4	2	100	1000	7.0	7.3	64	180	8.8	9.4	57	161
5	2	100	1000*	6.9	7.2	69		8.7	9.7	70	

* No thresholding imposed

To resolve this conundrum we have run a sample of 10 days, over the United States, where the complete wind processing scheme used both a 60 hour forecast and the normal 12 hour forecast (both valid at observation time). In this way we attempt to degrade the background field over the rawinsonde network where the verification is accomplished. The objective is twofold: to determine the sensitivity of the initial altitude assignment to the forecast quality; and to see if the rms statistics still display the same improvement as the influence of the forecast is increased. The statistical results for this experiment are also shown in Table 1. Several conclusions are apparent. It is seen that the accuracy of the vectors is decreased with the longer forecast, but the trend of the statistics as the auto-editor varies is similar to the shorter forecast experiments. With the relaxation on the initial pressure assignment there is again improvement in the CMV statistics, and improvement over the forecast increases, just as in the 12 hour case. The degree of pressure reassignment increases over the 12 hour forecast case, as would be anticipated, at least for cases 2 and 3 which are less extreme than case 4. Based on these results one might be tempted to accept a strong dependence on the forecast, even when poor, were it not for the evidence shown in Fig. 2. This figure presents scatter plots of the 12 hour vs. 60 hour forecast results for: initial height assignments, those reassigned with the operational variables (Case 2), and finally those reassigned as in Case 4.

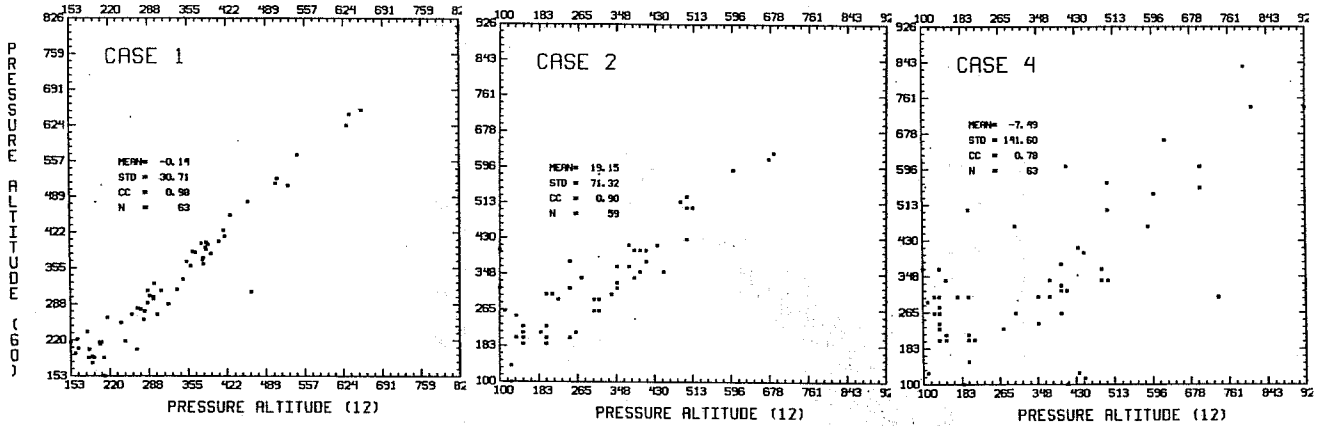


Fig. 2: Scatter plots of pressure altitude assignments obtained with 12 hour forecast processing vs. 60 hour forecast processing. Left: initial assignments. Center: auto-editor reassigned pressures using operation "best-fit" parameters. Right: auto editor reassigned pressures using relaxed "best-fit" parameters.

It is apparent that the initial height assignment is remarkably insensitive to the forecast. For the samples which pass both auto-editor tests (as displayed in Fig. 3) there is no bias difference and a standard deviation of only 30 hPa. (For the sample previous to the autoeditor the standard deviation is only 40 hPa.) This value is increased to 71 hPa for the operational reassigment and to 141 hPa for the relaxed function, numbers which are consistent with the changes to the initial assignments in each case, as given in Table 1.

Our immediate plan is to keep the operational scenario unchanged, despite the fact that rms statistics as compared to rawinsondes could be improved, as could the improvement to the forecast. This means further that the thresholding will be retained with a slight loss of sample. The small improvements in relaxing the fitting function do not seem worth the loss of independence from the forecast. There is another factor in support of this decision. If, for our full test sample of 10 days, the satellite vectors were assigned to the level of true best fit (i.e. the level where they best match the radiosonde by the same criteria used in (1) for the analysis match) the rms vector error is reduced from 8.6 to 4.9 ms^{-1} . At the same time the rms deviation of the altitude assignment is only 55 hPa and, as can be seen in Fig. 3, is quite random. Thus there appears to be little justification for letting the auto editor reassigment push the vectors all over the lot. They only need to be nudged the right way.

Our conclusion is that with our current operational system we can expect the normal match-up statistics to show approximate parity with the 12 hour forecast. However, as clearly shown by the results with the 60 hour forecast, the CMV could be having a significant positive impact where the forecast is poor. In a qualitative sense this may represent the true situation in data sparse areas.

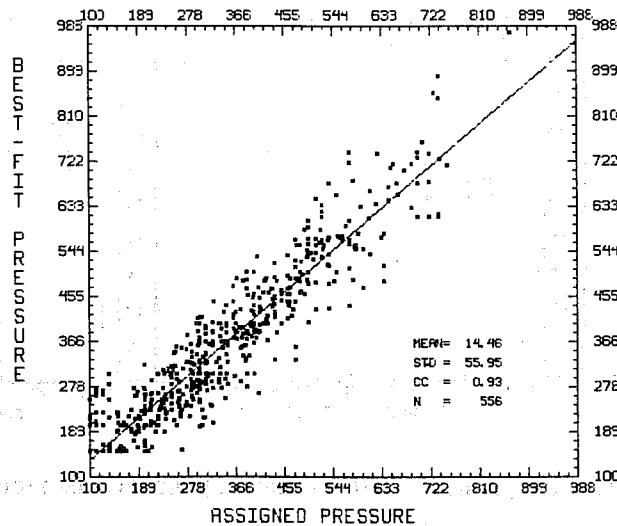


Fig. 3: Scatter plot of initial pressure altitude assignment vs. rawinsonde "best-fit" pressure for 10 day sample GOES-7 CMV, operational processing procedures.

5. VERIFICATION

Beginning in June NESDIS formalized the verification of the CMV by comparison to the rawinsonde into a routine operation. Match-up statistics are collected weekly for co-locations within 2 deg. latitude. GOES-7 and Meteosat CMV are derived from images collected 90, 60 and 30 minutes before synoptic time; Meteosat water vapor at 120, 90 and 30 minutes before. Thus all temporal co-locations are within 2 hours. Rawinsondes are required to report winds above and below the satellite assigned pressure and vectors are interpolated to that pressure. The match is accepted only if the rawinsonde reported within 25 hPa of the satellite assigned pressure altitude.

Fig. 4 and Table 2 give results of recent statistics. In Fig. 4 (top) the vector error of the three types of winds and the forecasts at the same location are shown for the autoedited sets. There is a suggestion that the GOES-7 product is best while the Meteosat water vapor product is worst. Based on our knowledge of the accuracy of their respective cloud altitude assignments this result would be expected. However, it is also obvious that the accuracy of all final products closely tracks that of the forecast, shown at the bottom of Fig. 4, so variations in the samples may mask their comparative merits. In Table 4 one sees that in virtually every instance the raw product (before the auto-editor) is much worse than the forecast. The quality is in all cases improved by the auto-editor, but rarely to the accuracy of the forecast. These results corroborate the experiments discussed in the previous section. The table also shows that the operational GOES are more likely to survive the editing process than either the Meteosat infrared or especially the Meteosat water vapor vectors. In this regard the superior quality of the initial pressure assignment using CO2 slicing is quite clear.

GOES 7 CD			FINAL PRODUCT			AUTOEDITED PRODUCT			HIGH-LEVEL WINDS			HIGH-LEVEL WINDS			RAW PRODUCT			HIGH-LEVEL WINDS												
			ALL WINDS			ALL WINDS			ALL WINDS			ALL WINDS			ALL WINDS			ALL WINDS												
			RMS			RMS			RMS			RMS			RMS			RMS												
			SAT			SAT			SAT			SAT			SAT			SAT												
			RAO			RAO			RAO			RAO			RAO			RAO												
			SPD			SPD			SPD			SPD			SPD			SPD												
			BIA			BIA			BIA			BIA			BIA			BIA												
			GSS			GSS			GSS			GSS			GSS			GSS												
			SAT			SAT			SAT			SAT			SAT			SAT												
			RAO			RAO			RAO			RAO			RAO			RAO												
			N			N			N			N			N			N												
15-May	6.6	6.2	-2.1	19.2	256	7.4	6.9	-2.4	22.5	164	7.1	6.3	-2.8	17.9	366	8.1	7.3	-3.2	21.6	222	8.3	6.2	-3.6	18.2	421	9.7	6.6	-4.3	20.7	247
22-May	6.9	6.9	-1.8	19.7	330	7.1	6.8	-1.5	22.0	238	6.9	6.8	-2.0	18.8	425	7.3	6.9	-1.8		298	10.0	6.7	-3.1	18.1	458	10.7	7.1	-3.8	20.7	311
29-May	7.5	7.6	-1.8	19.4	285	8.0	8.0	-2.1	22.7	187	7.4	7.0	-2.4	18.6	397	8.0	7.7	-2.5	21.3	271	10.1	7.5	-3.4	18.2	438	10.3	8.2	-3.7	20.6	297
5-Jun	7.0	8.2	-1.7	19.7	295	7.3	8.6	-1.8	21.7	234	7.2	7.8	-1.9	18.2	418	7.5	8.2	-2.1	20.2	319	9.8	8.2	-2.6	17.7	446	9.8	8.6	-3.6	20.1	327
12-Jun	7.2	6.9	-1.3	16.6	327	7.5	7.1	-1.3	18.0	267	6.9	6.9	-1.9	15.8	426	7.2	7.2	-1.8	17.4	342	9.4	6.7	-2.5	15.4	466	9.6	7.1	-3.1	17.2	360
19-Jun	7.8	8.4	-2.0	17.7	286	8.2	8.1	-2.2	19.2		7.6	7.3	-2.2	16.2	399	8.0	7.7	-2.4	17.8	317	9.9	7.1	-2.2	14.7	446	10.3	7.7	-2.8	16.3	332
26-Jun	6.8	6.8	-1.7	16.3	277	7.1	6.9	-1.5	17.2	211	7.2	6.8	-1.9	15.5	378	7.5	7.1	-1.9	16.4	289	9.5	6.8	-1.8	14.7	429	9.8	7.2	-2.1	15.5	334
3-Jul	7.2	8.4	-0.9	14.2	232	7.6	8.3	-0.5	14.8	178	7.3	7.8	-1.8	13.1	414	7.4	8.0	-1.5	13.3	334	9.3	7.2	-2.5	12.9	437	8.2	7.8	-2.5	13.0	343
10-Jul	7.0	6.8	-1.2	15.5	318	7.2	7.1	-1.4	16.5	257	7.2	6.7	-1.8	13.8	471	7.4	6.9	-1.8	14.3	376	9.0	6.3	-1.7	13.2	500	9.2	6.6	-2.3	14.0	388
17-Jul	7.1	7.7	-1.1	15.0	230	7.3	8.1	-1.1	15.8	188	7.2	7.8	-1.3	14.1	326	7.4	7.8	-1.5	15.0	283	9.2	6.2	-1.6	13.3	359	9.4	6.6	-2.0	14.1	282
24-Jul	7.1	7.0	-1.1	14.1	138	7.0	7.2	-1.0	14.1	121	7.2	7.0	-1.9	14.1	226	7.4	7.3	-1.9	14.7	189	9.3	6.8	-2.3	13.7	240	9.2	7.2	-2.8	14.4	193
31-Jul	6.8	6.4	-2.0	16.2	268	7.2	6.7	-1.7	17.5	190	6.9	6.2	-2.2	15.2	351	7.3	6.7	-2.1	16.4	252	9.5	6.3	-2.8	15.0	385	10.1	6.9	-3.4	16.2	275
7-Aug	6.6	6.3	-1.7	15.7	327	7.0	6.6	-1.7	17.5	252	6.5	6.0	-1.8	14.6	450	6.9	6.4	-1.9	16.2	342	8.9	6.0	-2.1	14.1	460	9.2	6.4	-3.0	15.8	323
14-Aug	6.6	6.2	-0.4	14.9	295	6.7	6.4	-0.4	16.0	241	7.0	6.3	-1.2	14.2	422	7.3	6.8	-1.2	15.5	333	8.2	6.4	-1.8	13.8	460	9.6	6.7	-2.5	15.5	346

METEOSAT 3 CD			AUTOEDITED PRODUCT			RAW PRODUCT			HIGH-LEVEL WINDS			HIGH-LEVEL WINDS			RAW PRODUCT			HIGH-LEVEL WINDS																					
			ALL WINDS			ALL WINDS			ALL WINDS			ALL WINDS			ALL WINDS			ALL WINDS																					
			RMS			RMS			RMS			RMS			RMS			RMS																					
			SAT			SAT			SAT			SAT			SAT			SAT																					
			RAO			RAO			RAO			RAO			RAO			RAO																					
			SPD			SPD			SPD			SPD			SPD			SPD																					
			BIA			BIA			BIA			BIA			BIA			BIA																					
			GSS			GSS			GSS			GSS			GSS			GSS																					
			SAT			SAT			SAT			SAT			SAT			SAT																					
			RAO			RAO			RAO			RAO			RAO			RAO																					
			N			N			N			N			N			N																					
7.3	7.1	-1.5	21.8	64.0	8.0	8.0	-1.3	26.6	45	11.3	5.9	-4.0	17.0	88	12.8	7.1	-7.3	21.8	44	8.4	7.9	-1.5	21.6	84	8.8	8.4	-1.4	24.3	66	12.8	7.5	-0.8	19.1	142	13.1	7.5	-1.0	19.6	128
8.0	7.8	-2.2	21.0	150.0	8.6	8.5	-2.1	22.8	118	10.8	6.6	-1.0	16.4	207	11.1	7.9	-3.9	20.0	106	7.6	6.6	-1.4	18.3	119	7.5	6.7	-1.2	18.2	114	11.0	6.0	-1.5	15.7	184	10.9	6.0	-1.4	15.7	182
9.0	7.8	-1.9	17.2	125.0	8.4	8.3	-1.9	19.4	98	12.2	6.5	-0.8	13.5	200	12.8	7.2	-2.4	16.0	124	8.7	8.7	0.6	13.7	27	8.9	8.9	0.6	14.1	26	10.3	6.8	-0.2	12.0	57	10.3	6.7	0.1	12.4	54
6.8	6.9	-1.4	19.6	143.0	7.0	7.3	-1.6	21.6	121	11.7	6.4	-0.4	15.1	261	10.8	7.2	-2.9	10.0	179	8.7	7.0	-0.8	14.6	84	6.6	7.0	-0.8	14.7	82	11.0	6.0	-1.5	15.7	184	10.9	6.0	-1.4	15.7	182
7.2	6.9	-1.8	17.7	159.0	7.2	7.1	-1.6	19.2	129	10.6	6.3	-0.9	13.7	236	10.0	9.9	-2.2	15.3	190	8.5	7.2	-0.9	17.5	78	8.8	7.3	-0.8	17.7	76	12.4	6.7	-0.2	15.1	142	12.4	6.7	0.3	15.1	141
8.4	7.7	-1.1	16.4	132.0	8.8	8.3	-1.1	18.0	106	10.7	6.2	-0.8	13.1	195	10.0	6.8	-2.1	14.8	133	7.0	5.5	-0.8	12.0	83	7.0	5.6	-0.8	12.0	81	9.5	5.4	-1.4	10.8	164	8.5	5.4	-1.4	10.8	163
7.3	7.0	-1.1	16.1	126.0	7.5	7.1	-1.1	16.6	115	8.8	6.4	-1.3	13.3	208	8.5	8.8	-2.1	14.3	177	7.8	6.7	-1.2	15.1	62	7.9	6.7	-1.2	14.9	59	11.0	6.2	-0.4	14.8	94	11.0	6.2	-0.4	14.8	94
7.4	7.3	-1.8	17.8	123.0	7.9	8.0	-2.0	19.7	100	10.1	6.5	-1.3	15.1	172	9.9	7.3	-2.7	17.3	129	9.4	8.6	-3.8	24.0	38	8.5	8.7	-3.7	24.2	37	12.5	6.4	-1.0	18.3	83	12.5	6.4	-1.0	18.3	83
9.0	8.7	-3.2	18.8	79.0	9.6	9.3	-3.8	20.5	66	11.0	6.4	-2.0	14.5	162	10.9	7.3	-4.6	16.8	111	9.2	6.7	-1.0	16.3	38	9.2	8.9	-0.9	16.4	37	11.5	5.7	-1.9	13.1	54	11.5	5.7	-1.9	13.1	54
7.7	6.8	-1.4	17.4	127.0	8.1	7.2	-1.5	18.7	108	10.8	7.5	-3.2	16.1	192	11.4	8.4	-4.7	18.6	134	10.1	8.6	-2.9	22.2	39	10.1	8.6	-2.9	22.2	39	12.1	6.7	0.6	17.9	73	12.1	6.7	0.6	17.9	73
6.9	6.8	-2.2	16.9	129.0	7.4	7.4	-2.4	18.8	99	10.8	7.1	-3.5	15.2	259	11.9	7.9	-5.2	18.3	191	8.8	7.7	-1.8	17.8	62	8.9	7.7	-1.8	17.9	61	11.9	5.7	-0.2	13.9	155	11.9	5.7	-0.2	13.9	155
6.9	6.5	-0.6	15.9	86.0	7.5	7.1	-0.9	17.8	67	12.1	7.7	-3.0	15.1	199	13.3	8.7	-5.0	18.2	148	8.3	7.4	-2.3	13.7	63	8.3	7.4	-2.3	13.6	62	10.1	5.6	-0.7	11.2	170	10.1	5.6	-0.7	11.2	170

Table 2: 12 Weeks of statistical comparisons between CMV and rawinsondes. NESDIS operational GOES-7 and NESDIS research Meteosat infrared and water vapor are presented. Samples are segregated as "all" and high (<400 hPa), and before and after application of auto-editor. Units are ms⁻¹.

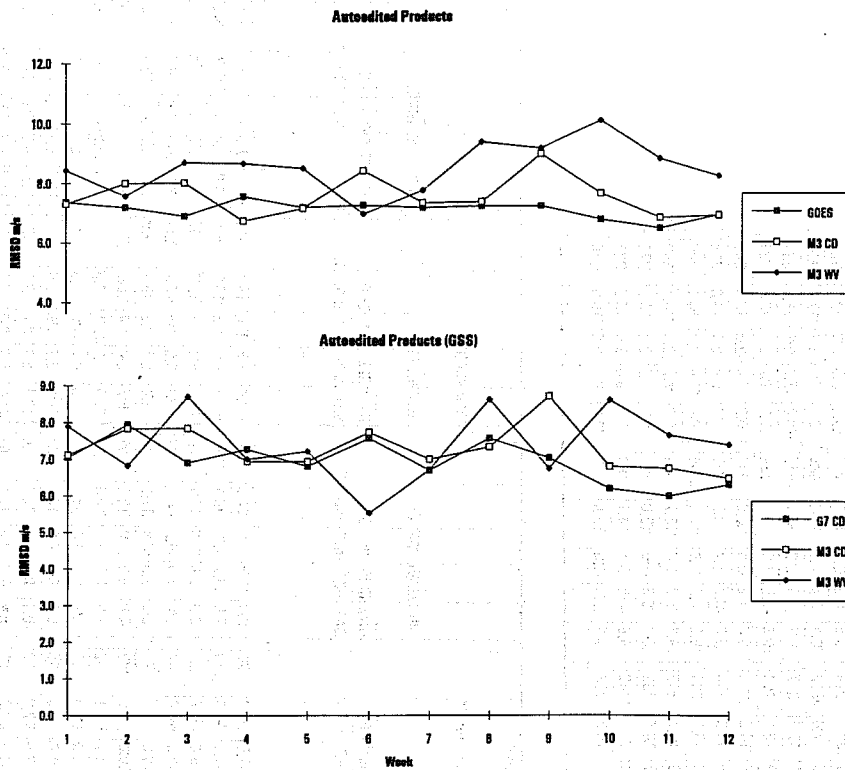


Fig. 4: 12 weeks of verification statistics (vector error as compared to rawinsondes) for GOES-7 infrared, Meteosat infrared, and Meteosat water vapor CMV. Top: statistics for auto-editor processed samples. Bottom: coincident error of NMC 12 hour forecast. Units are ms^{-1} .

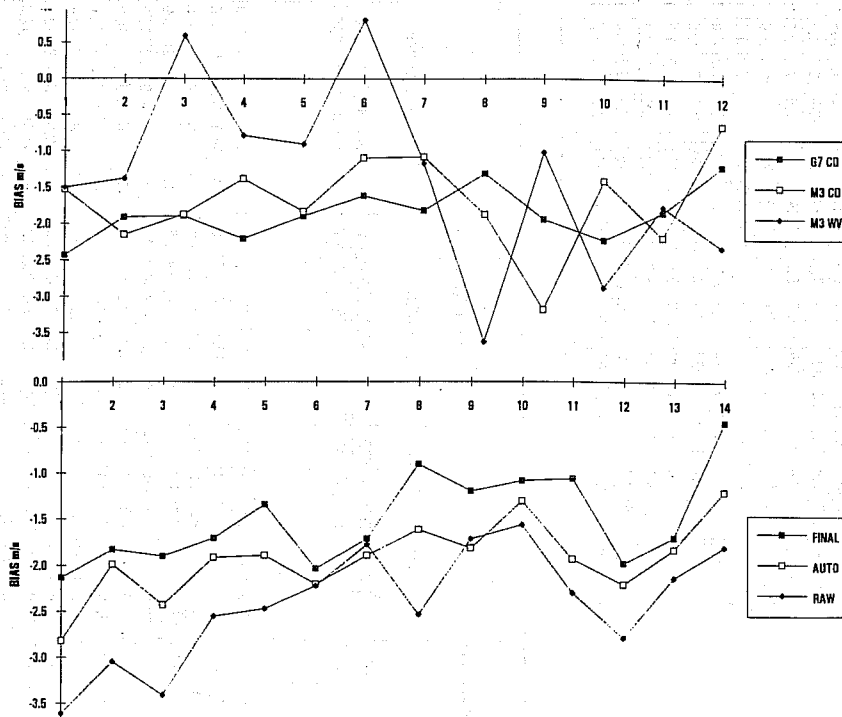


Fig. 5: Top: Bias statistics corresponding to samples of Fig 4. Bottom: Improvements in bias errors of GOES-7 CMV made by auto-editor and manual editing (Final).

Fig 5 presents speed bias statistics for the auto-edited winds. With the exception of two weeks for the water vapor, all sets demonstrate the well-known slow bias with respect to rawinsondes. Although not shown here, the bias of the forecast is also slow, but much less so than the satellite vector's. The bottom of Fig. 5 shows that the bias is somewhat improved by the auto-editor, but remains substantial. The experiments described in Section 3 suggest that it could be slightly further improved by fitting more tightly to the guess, but only slightly. The current version of the auto-editor does not do well in correcting this deficiency. It is interesting to note that the manual editing manages to reduce the bias error slightly further, although it does not (see Final vs. Autoedited columns for GOES-7 CD in Table 2) consistently reduce the vector error. We have no explanation for this.

6. GRADIENT WIND ESTIMATES FROM VAS

Gradient winds are produced four times daily (to coincide with the cloud-drift wind vectors) from VAS soundings which cover the latitude extent 23 - 49 N. Temperature/moisture profiles are attempted at a density of every 20 VAS fov (but using the standard 11 x 11 fov averaging). This is equivalent to a grid mesh of approximately 160-170 km but filled only in the cloud-free areas. One innovation of the current retrieval method is the introduction of an "area" of AVHRR-derived sea-surface temperature at a resolution of about 20 km. This has improved the cloud discriminating algorithm considerably over the ocean, especially for the detection of low stratus. Unfortunately, low stratus is prevalent over large regions of the Pacific, as can be seen in the infrared imagery shown in Fig. 6, and consequently only a few retrievals are obtained. A topic of future research is the development of an algorithm for deriving gradient wind estimates over low stratus, since coverage could be so much improved.

Temperature/moisture profiles are converted to geopotential thickness and anchored to an objective analysis of the 1000 hPa geopotential to derive vertical profiles of geopotential. These are subsequently analyzed with a 2-dimensional recursive filter objective analysis using the NMC global (aviation) forecast (12 hour for 00 and 12 UTC and 06 hour for 06 and 18 UTC) as a background. The analyses are produced at a 1.2 degree latitude/longitude spacing with fairly liberal smoothing specified as an analysis parameter.

Gradient winds are calculated using derivatives obtained from a least squares fit of a second degree polynomial geopotential surface to the 25 points centered on the grid point closest to each successful VAS retrieval. Thus the gradient wind is representative of a surface over about 6 * 6 degrees.

An objective estimate of the quality of each geopotential datum is a product of the analysis system. The estimate, scaled 0-100, has this year been reworked to be a combination of the "fit" of the datum to the final analysis, the density of neighboring observations, and a subjective evaluation of the background field based solely on location. A quality threshold (currently 60) is used to determine if the

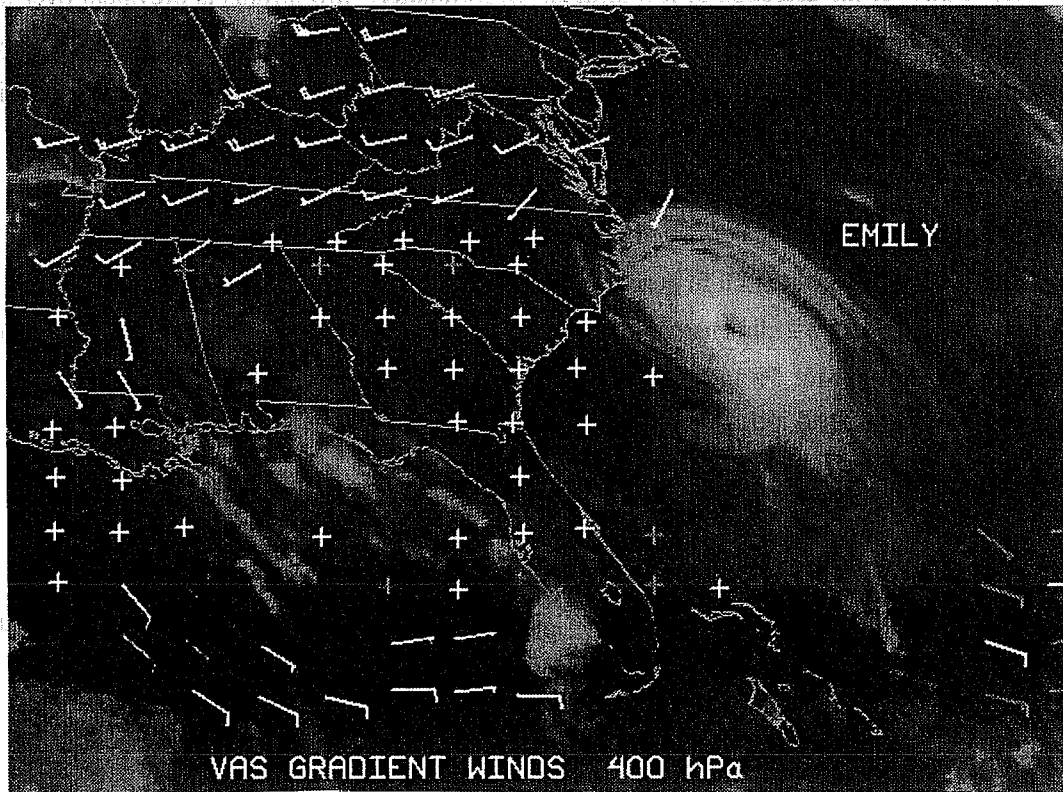
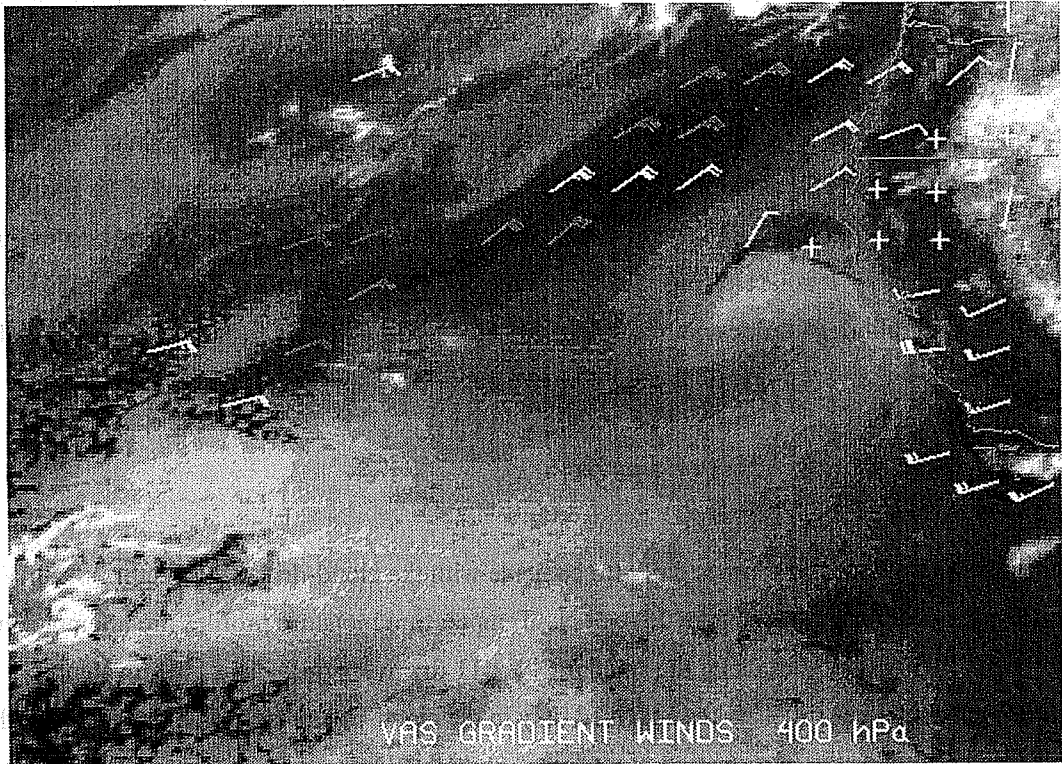


Fig. 6: Gradient wind estimates obtained over eastern Pacific and western Atlantic, August 31, 1993.

wind is to be passed to the NMC. Subjectively the quality flagging is reasonable. Reports which cannot determine a gradient, i.e. isolated reports, reports in clear "slots" or reports near the edge of clouds, are more prone to rejection. An example of the current product is given in Fig. 6. The stratus problem over the Pacific is very obvious. Over the Atlantic we are limited by our local zenith angle restriction which prevented good coverage around Hurricane Emily. Observation plotted in a darker shade are those failing the quality threshold.

Table 3. August 93 statistics of NESDIS VAS gradient winds versus rawinsondes (R). Statistics calculated for gradient winds generated from NMC 12 hour forecasts (Fcst) and radiosonde analyses (A) are also given. Units are ms^{-1} .

RMS Vector Error			
P	FCST-R	VAS-R	A-R
850	6.0	5.3	5.4
700	5.5	5.2	4.9
500	6.5	6.0	5.7
400	7.3	6.4	6.3
300	9.4	7.9	7.9

Mean Speed				
P	FCST	VAS	A	R
850	4.0	5.1	4.7	6.8
700	4.9	6.1	5.4	6.4
500	6.5	7.6	6.9	8.2
400	7.9	9.1	8.3	9.7
300	9.8	11.2	10.3	12.2

Table 3 gives a statistical comparison for a sample of VAS gradient winds compared to rawinsondes during August 1993. Comparisons at the same (VAS) locations are also shown for gradient winds generated from the forecasts and from analyses of the radiosonde geopotentials. In terms of the vector rms, the VAS is a clear improvement over the forecast product, particularly at higher levels, and is approximately equivalent to the radiosonde geopotential analysis product. In terms of average speed only, the VAS is significantly more accurate than both the forecast and the radiosonde analysis. These results again confirm (Hayden, 1992) that the satellite retrievals can be processed to offer useful information on the gradient of the geopotential. The National Meteorological Center has accepted this

result and requested additional processing in the southern hemisphere. Unfortunately, the time available for VAS processing in the GOES-7 schedule makes this difficult. However, a pilot program is scheduled for winter 93-94.

7. DISCUSSION AND CURRENT RESEARCH

Our experience over the past year and a half has established that the automatic generation of winds from either the infrared or the water vapor imagery is viable when combined with the auto-editor. It is discouraging that we still do not show consistent improvement over the 12-hour numerical forecast, but we have demonstrated above, by degrading the forecast, that it is quite possible that we are improving on forecasts in data sparse areas. We have also demonstrated that the gradient wind estimates from temperature soundings are potentially useful. They improve on the geopotential gradient estimates of the forecast. However, if used as pseudo winds the vector errors are substantial, far larger than the cloud drift winds. Clearly they should be assimilated as gradients and not winds. We have examined the sensitivity of verification statistics as a function of pressure altitude assignment to justify the selection of parameters for the operational auto-editor. We have concluded that it is desirable not to deviate too greatly from the initial assignment, even if the accuracy appears to improve. This conclusion applies only to CMV with initial heights specified by CO₂ slicing and may need modifying when that method is not available. Certainly the height assignment for the water vapor vectors (away from cloud) is a poorly posed problem which needs to be addressed.

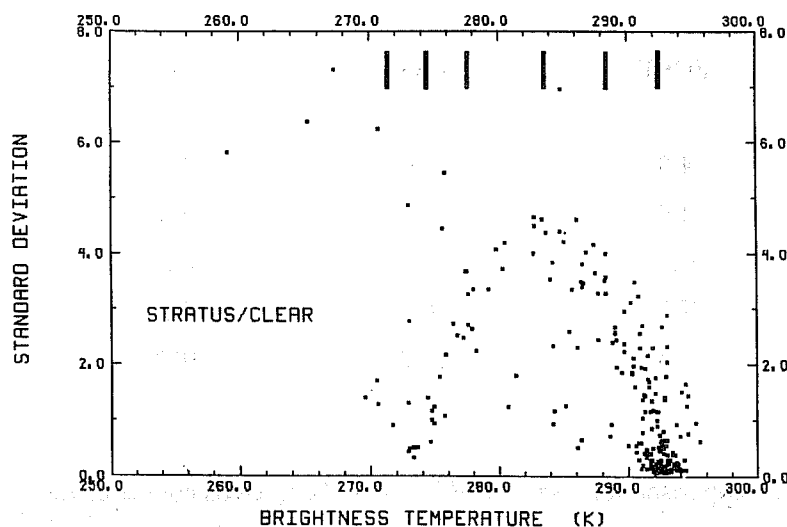


Fig. 7: A Coakley diagram of infrared brightness temperatures plotted against 3 x 3 standard deviations.

The persistent slow bias error in GOES processing is not significantly mitigated by the auto-editor. According to published statistics it is a larger problem in the NESDIS processing than in the European or Japanese. We find this quite annoying and have been investigating two avenues to correct this

deficiency. The first is directed to target selection. We propose to use the clustering logic already on hand for the water vapor height assignment to refine the target choice. The clustering is combined with the Coakley coherence test (Coakley, 1983) to avoid multiple layer clouds and, possibly, to isolate small cirrus tracers. For example, consider the diagram shown in Fig. 7 where the window radiance temperature is plotted against the standard deviation of the adjacent 3 x 3 fov taken over the complete target box. A simple, single cloud layer situation will give the familiar "arch" with warm and cold feet representing cloud and clear areas. The cluster analysis can be used to examine the fidelity of the arch.

Other restrictions can be imposed. For example:

- o a fixed percentage of scenes can be required to exceed a standard deviation threshold (y-axis) to avoid a uniform scene.
- o a fixed minimum and maximum percentage of the remaining scenes may be assigned to categorize the size of the tracer.

Finally our plan is to use all cluster tests and height assignments on the targets in each image, not just the first, to ensure coherence. This procedure has been investigated by Santai and Desbois (1993) but not in the CIMSS/NESDIS research.

A second approach to improving the slow bias is to modify the auto-editing procedure. Recent testing with the sample discussed in Section 3 has been very promising. Results of a four day test using the operational and an updated version of the auto-editor are shown in Fig. 8 and Table 4. Fig 8 (left) shows the bias error as a function of rawinsonde wind speed for both the operational and experimental editors. For these results the normal 12 hour forecast was used. The operational results show the typical trend of a slow bias increasing as the wind speed increases. The experimental results show a marked improvement. The regression line is nearly horizontal. Table 4 presents verification statistics for this experiment with the 12 hour forecast and also for the degraded, 60 hour forecast. The improvement offered by the new version of the editor is dramatic. The removal of the large negative bias is successful. The sample size of retained CMV is increased over that of the operational editor. The vector error is reduced. All of these improvements hold for the degraded forecast as well. And most importantly, the new editor improves significantly over the 12 hour forecast, a goal we have striven after for many unsuccessful years.

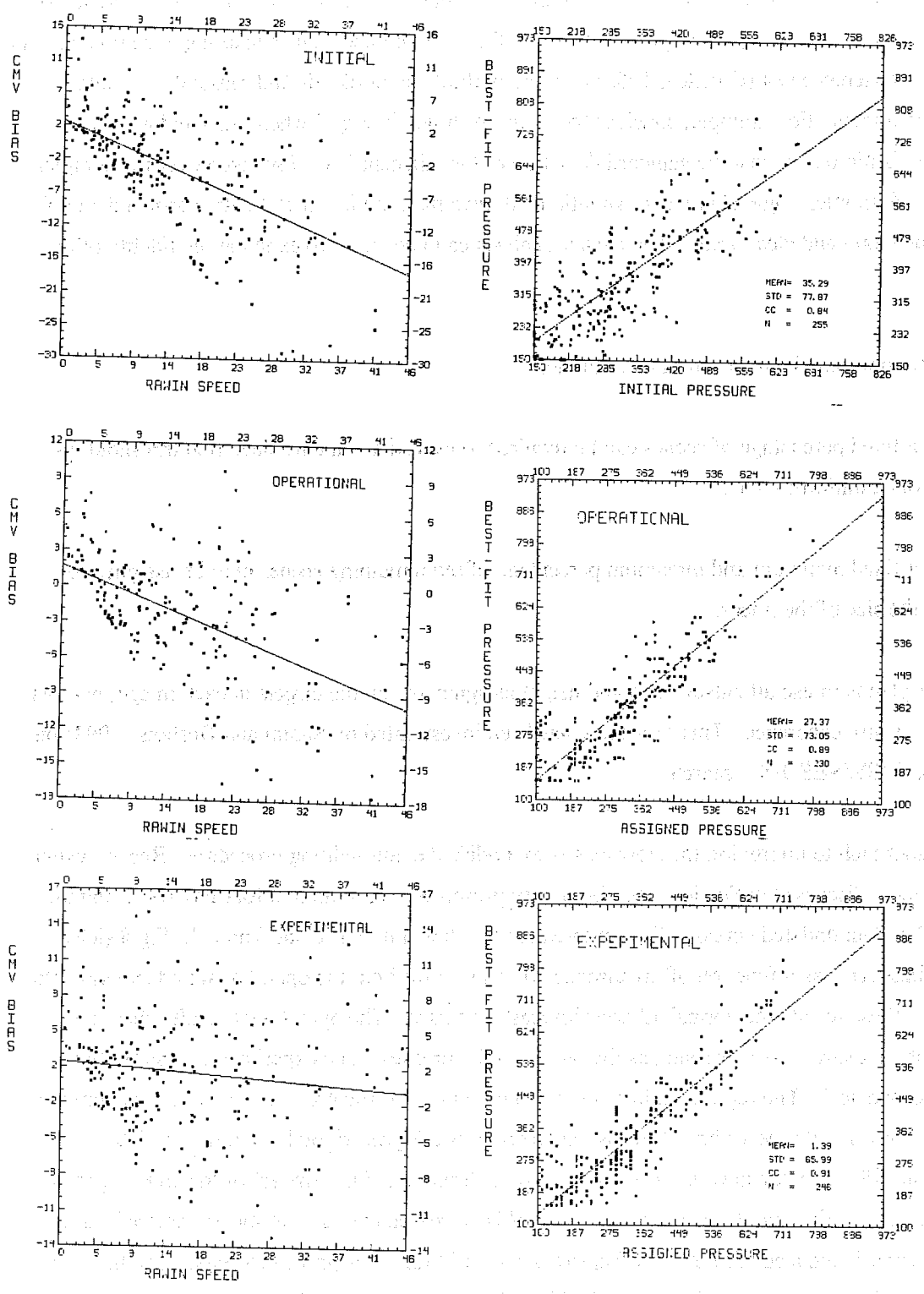


Fig. 8: Left: Scatter diagrams of CMV speed bias vs. rawinsonde speed for initial pressure altitude assignment and after processing with operational and experimental editors. Right: Scatter diagrams of pressure altitude assignment v. level of best fit as determined from rawinsondes.

Fig. 8 (right) compares the pressure altitudes of the three assignments (initial, operational and experimental editor) with the pressure of the level of best fit (for the sample using the 12 hour forecast). It can be seen that the initial assignments have a bias of 35 hPa, and the higher the assigned pressure, the more erroneous (assigned too high). The operational editor partially corrects these deficiencies, removing the pressure dependent trend, but only reducing the bias to 27 hPa. The experimental editor removes the bias almost completely, leaving a value of only 1 hPa. The standard deviation of the difference between assigned and "best-fit" levels also improves from an initial 77 to 73 and finally to 66 hPa.

These satisfying conclusions are based on only four cases and are therefore tentative. The days were chosen because the initial assignments showed larger than usual errors (compare Fig. 4 and 9) and may somewhat overstate the improvement. However, we have no reason to believe that they are not representative. Further experiments on other (than GOES-7) data sets need to be accomplished, and their synoptic situations need to be investigated. In the meantime we shall initiate a parallel operational run using the experimental editor.

Table 3. Rawinsonde match statistics comparing CMV pressure altitude assignments initially and after processing with the Operational and Experimental editors. Results are shown for the normal (12-hr) and a degraded (60-hr) background (Fcst). Units are ms^{-1} .

	12-hr						60-hr				
	Rms			Bias			Rms		Bias		
	CMV	Fcst	N	CMV	Fcst		CMV	Fcst	N	CMV	Fcst
Init	10.0	6.7	255	-3.9	-0.7		10.8	10.1	250	-4.4	-1.5
Oper	8.0	7.2	230	-2.7	-1.0		8.8	9.8	211	-3.6	-2.1
Exp	7.8	8.5	246	1.0	-0.1		8.6	9.5	235	-0.9	-0.8

REFERENCES

Coakley J. and D. G. Baldwin, 1983: Towards the Objective Analysis of Clouds from Satellite Imagery Data. *J. Clim and Appl. Meteor.* 23, 1065-1099.

Hayden, C. M. and R. T. Merrill, 1988: Recent NESDIS research in wind estimation from geostationary satellite images. ECMWF Seminar on Data Assimilation and the Use of Satellite Data, 5-8 September.

Hayden, C. M. and R. J. Purser, 1988: Three-dimensional recursive filter objective analysis of meteorological fields. Eighth Conference on Numerical Weather Prediction, February 22-26, Baltimore, MD, AMS.

Hayden, C. M. and C. S. Velden, 1991: Quality control and assimilation experiments with satellite derived wind estimates. Preprint Volume of 9th Conference on Numerical Weather Prediction Oct 14-18, Denver, CO, Amer. Meteor. Soc., 19-23.

Hayden, C. M., 1991: Research leading to future operational methods for wind extraction. Workshop on wind extraction from operational meteorological satellite data, 17-19 September 1991. EUM P 10, ISBN 92-9110-007-2, 161-169.

Hayden, C. M., W. P. Menzel, S. J. Nieman, and T. J. Schmit, 1992: Recent progress in methods for deriving winds from satellite data at NESDIS/CIMSS. to be published-COSPAR, 4 September 1992, Washington D.C.

Merrill, R. T., 1989: Advances in the automated production of wind estimates from geostationary satellite imagery. Fourth Conference on Satellite Meteorology and Oceanography, May 15-19, San Diego, CA, AMS.

Menzel, W. P., W. L. Smith and T. R. Stewart, 1983: Improved cloud motion wind vector and altitude assignment using VAS. J. Clim. Appl. Meteor., 22, 377-384.

Nieman, S. J., J. Schmetz and P. Menzel, 1992: A comparison of several techniques to assign heights to cloud tracers. Submitted to J. Appl. Meteor.

Schmetz J., K. Holmlund, B. Mason, J. Hoffman, and B. Strauss, 1992: Operational Cloud Motion Winds from METEOSAT Infrared Images. Submitted to J. Appl. Meteor.

Santai A. and M. Desbois, 1993: Construction of cloud trajectories to study the cloud life cycle. to be published-COSPAR, 4 September 1992, Washington D.C.

Szejwach, G. 1982: Determination of semi-transparent cirrus cloud temperatures from infrared radiances: application to Meteosat. J. Appl Meteor., 21, 384-392.

Velden C. and S. Nieman, 1993: Tracking motions from satellite water vapor imagery: quantitative applications to hurricane track forecasting. Preprint Volume, 20th Conference on Hurricanes and Tropical Meteorology, 10-14 May 1993, San Antonio, TX, 193-196.